Supporting Information for

Glass Transition Temperature of Conjugated Polymers by Oscillatory Shear Rheometry

Renxuan Xie[1], Youngmin Lee[1], Melissa Aplan[1], Nick Caggiano[1], Christian Müller[2], Ralph H. Colby[1,3], Enrique D. Gomez[1,4]**

[1]Department of Chemical Engineering, The Pennsylvania State University, University Park, PA 16802
[2]Department of Chemistry and Chemical Engineering, Chalmers University of Technology, 41296 Göteborg, Sweden
[3]Department of Materials Science and Engineering, The Pennsylvania State University, University Park, PA 16802
[4]The Materials Research Institute, The Pennsylvania State University, University Park, PA 16802

1. Differential scanning calorimetry (DSC) for RR P3HTs

RR P3HTs were first melted at 260 ˚C and then cooled to -40 ˚C at 20 ˚C /min in the DSC under nitrogen. Figure S1a shows the second heating scans, with clear melting transitions for RR P3HTs between 220 and 240 ˚C, except for RR P3HT **1** (not shown), which melts at 160 ˚C. A subtle step change for a transition in between -10 and 20 ˚C is also visible. Figure S1b shows the derivative curves from (a), potentially indicating a glass transition in the aforementioned temperature range.

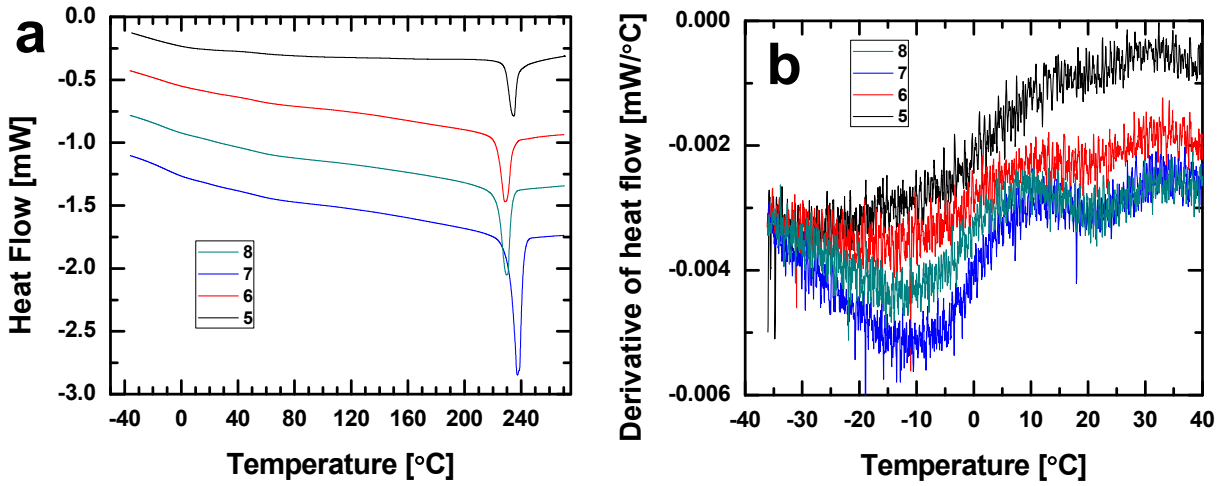

Figure S1. (a) Second heating scans of RR P3HTs at 20℃/min from DSC. Data is vertically shifted for clarity. (b) Derivative of heat flow shown in (a). Characteristics of polymers 5 through 8 can be found in Table 1 of the main text.

2. Differential refractive index (dn/dc) and dielectric constant for P3HTs

Figure S2 shows the difference in polarizability between RR and RRa P3HTs in solution and the difference in dielectric constant in the melt. The larger *dn/dc* value for RR P3HT in chlorobenzene suggests it is more polarizable than RRa P3HT; this is consistent with the higher dielectric constant of RR P3HT at -40 ˚C (below T_g). *dn/dc* is calculated to be 0.179 and 0.155 ml/g for RR P3HT and RRa P3HT, respectively, from the slopes of the lines shown in Figure S2a. The dielectric constants extracted from dielectric relaxation spectroscopy (DRS) for **RRa 3**, **RRa 4**, RR **7** trial 1, and RR **7** trial 2 at 1 MHz are 2.77, 2.87 3.21 and 3.28, respectively.

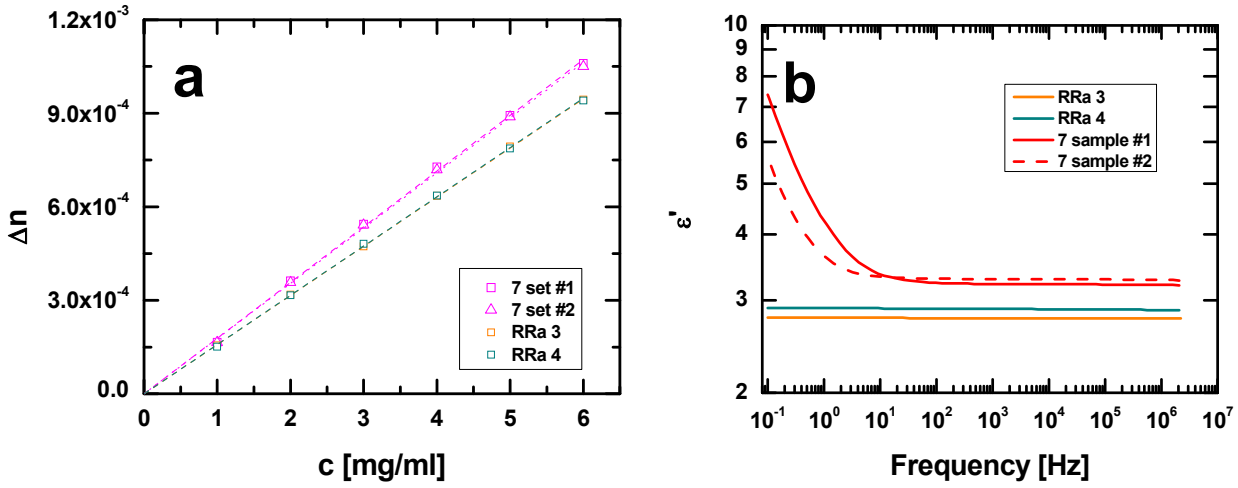

Figure S2. (a) Difference in refractive index versus concentration for RR P3HT **7** (2 sets of solutions), **RRa 3**, and **RRa 4** in chlorobenzene at 30.0 ˚C at a wavelength of 620 nm. (b) Frequency dependence of the real permittivity (ε') for RR P3HT **7** (amplitude of 0.5 V) and **RRa 3** & **4** (amplitude of 1.5 V) at -40 ˚C from DRS.

3. Gel permeation chromatography (GPC) traces for P3HTs and PFTBT

Figure S3 shows the GPC traces for all P3HTs used in this work. The observed bimodal distribution might originate from pushing the reaction to near completion to maximize the yield, such that the reaction is mostly terminated by recombination. Nevertheless, RRa P3HT shows only one broad distribution.

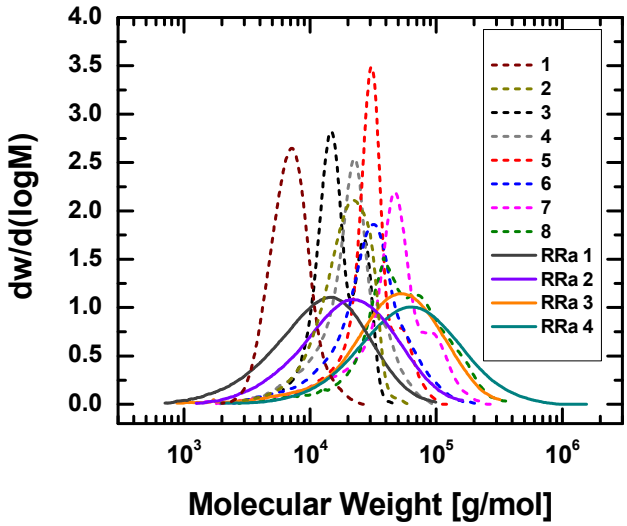

Figure S3. GPC traces of RR P3HTs **1, 2, 3, 4, 5, 6, 7, 8** and **RRa P3HTs 1, 2, 3, 4** in chlorobenzene at elevated temperature whose characteristics are shown in Table 1 of the main text.

PFTBT is less soluble than P3HT, possibly due to its smaller mass fraction of alkyl side chain. Thus, a high temperature GPC (Agilent PL-GPC 220) coupled with a sample preparation system (Agilent PL-SP 260VS) was used to determine the molecular weight distribution. In Figure S4, all PFTBTs show large dispersity with bimodal distributions.

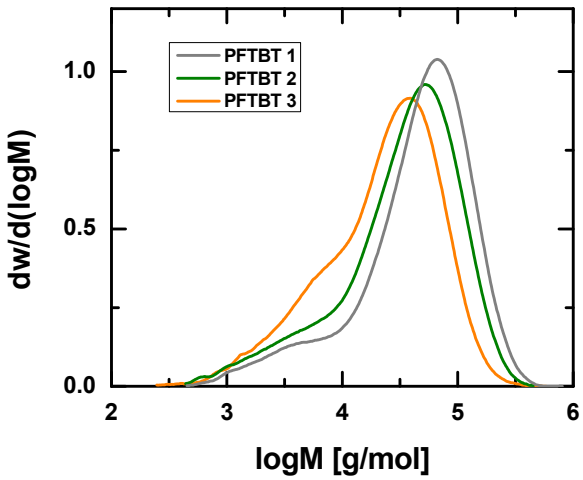

Figure S4. GPC traces of **PFTBTs** in 1,2,4-trichlorobenzene at 150 ˚C determined from a universal calibration that relies on refractive index and viscometer detectors.

4. Backbone glass transition temperature (T_α) determined by DRS for RRa P3HT

Glass transition temperatures were also obtained by Dielectric Relaxation Spectroscopy (DRS). We compare T_g from DRS with the rheology results shown in Figure 5 of the main text. Only the main backbone glass transition (α process) is visible from DRS for RRa P3HT as shown in Figure S5 below. The alkyl side chain glass transition (α_{PE} process) is not detectable due to the lack of a dipole moment on the side chain. In addition, the α process for RR P3HT is masked under its mixed ionic (due to impurities) / electronic conductivity response, which is about three orders of magnitude higher than that of RRa P3HT. Therefore, the dielectric loss peak is modeled only

for RRa P3HT. We use the Havriliak−Negami (H-N) function[1], from which the peak frequency (ω_{max}) is extracted at each temperature. T_α is then extrapolated from the classic Vogel−Fulcher−Tammann (VFT) fit[2] of ω_{max}.

$$\text{H-N:} \quad \epsilon^* = \epsilon_\infty + \frac{\Delta\epsilon}{(1+(i\omega\tau)^\alpha)^\beta} \tag{2}$$

$$\text{VFT:} \quad \omega_{\max} = \omega_\infty \exp\left(-\frac{DT_0}{T-T_0}\right) \tag{3}$$

T_α's are determined to be 262 K, 271 K, 274 K and 278 K for **RRa 1**, **RRa 2**, **RRa 3** and **RRa 4** P3HTs, respectively. These values are within 3 degrees of the values obtained from rheology (Figure 5 of the main text and Table S2 below). The VFT fitting parameters for RRa P3HTs are summarized in Table S1 below.

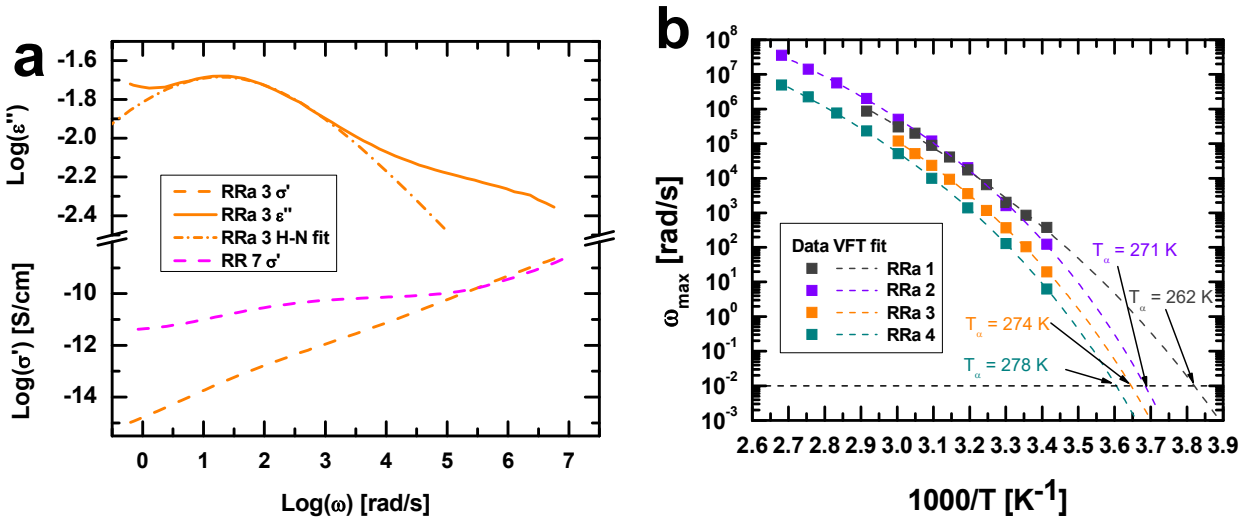

Figure S5. (a) Frequency dependence of the dielectric loss (ε'') and the in-phase conductivity (σ') for **RRa 3** and RR **7** P3HTs at 20 ˚C from 10^7 to 0.63 rad/s. The H-N function is used to fit the α relaxation (ε'' peak) for **RRa 3** P3HT, and ω_{max} and the dielectric strength (Δε) are extracted. (b) T_α's are determined to be 262 K, 271 K, 274 K and 278 K for **RRa 1**, **RRa 2**, **RRa 3** and **RRa 4** P3HTs, respectively, by extrapolating the VFT fits of the ω_{max} to 0.01 rad/s.

Table S1: Fitting parameters of Equation (3) for α transition of RRa P3HT by DRS

	ω_∞ [rad/s]	D [-]	T_0 [K]
RRa 1	5.3 x 10^{13}	2833	184
RRa 2	9.7 x 10^{12}	2003	213
RRa 3	6.5 x 10^{12}	2209	210
RRa 4	6.5 x 10^{12}	2283	211

5. Insitu heating WAXS of PFTBT

In-situ heating wide angle X-ray scattering (WAXS) was carried out at beamline 7.3.3 of the Advanced Light Source in Lawrence Berkeley National Laboratory. Figure S6 shows the circularly-averaged intensity of **PFTBT 2** at various temperatures. At room temperature, two broad peaks are visible at 0.4 $Å^{-1}$ and 1.4 $Å^{-1}$. The halo at 0.4 $Å^{-1}$ corresponds to the average interchain spacing, suggesting PFTBT is nanophase separated into backbone and alkyl side chains domains. Nevertheless, the volume of alkyl side chain nanodomain may not be large enough to exhibit its own T_g at around -100 ˚C, in contrast with P3HTs. Alternatively, the side chain T_g may be below -120 ºC, making it inaccessible for our rheology measurements. As temperature increases, the cold crystallization process starts around 160 ˚C and then the crystalline peaks are fully developed at 190 ˚C. This process is consistent with the rheology measurements shown in Figure 7 of the main text.

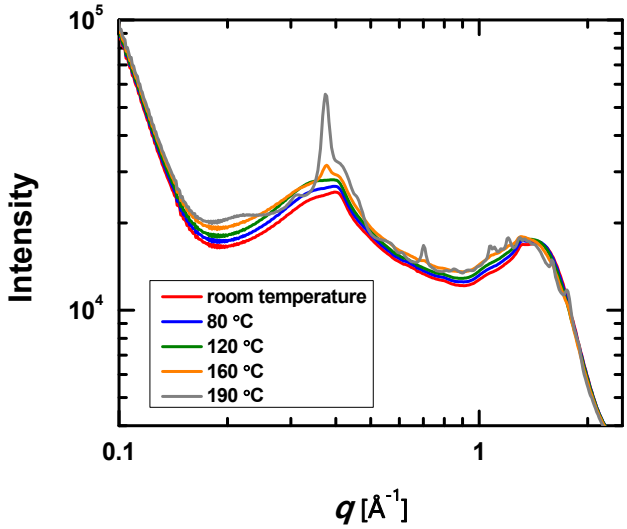

Figure S6. In-situ heating WAXS data for **PFTBT 2** that was previously quenched from 270 ˚C to room temperature in the rheometer.

6. Glass Transition Temperature Summary for P3HT

Table S2. **Summary of glass transition temperatures for all P3HTs studied in this work**

P3HTs	1	2	3	4	5	6	7	8	RRa 1	RRa 2	RRa 3	RRa 4
M_n [kg/mol]	2.7	5.3	14.5	15.3	24.2	21.5	27.7	36.6	5.5	12.3	41.7	44.9
T_α* ± 1.5 [˚C]	-5.3	-1.4	1.4	3.4	9.6	9.9	10.9	14.2	-12.2	-4.5	3.8	6.3
$T_{\alpha PE}$* ± 2.0 [˚C]	-	-	-101	-102	-99	-104	-102	-101	-97	-95	-95	-93
T_α by DRS ± 2.0 [˚C]	-	-	-	-	-	-	-	-	-11.4	-1.8	1.2	4.4

*determined by the peak of G'' from rheology at 10 rad/s, 5 ˚C/min heating and strain amplitude of 0.001.

7. References

(1) Havriliak, S.; Negami, S. *Polymer* **1967**, *8*, 161–210.

(2) Rault, J. *J. Non. Cryst. Solids* **2000**, *271*, 177–217.